
Lymph Node Staging with a Combined Protocol of ¹⁸F-FDG PET/MRI and Sentinel Node SPECT/CT: A Prospective Study in Patients with FIGO I/II Cervical Carcinoma

Matthias Weissinger¹, Florin-Andrei Taran², Sergios Gatidis³, Stefan Kommos⁴, Konstantin Nikolaou^{3,5,6}, Samine Sahbai¹, Christian la Fougère^{1,5,6}, Sara Yvonne Brucker^{*4}, and Helmut Dittmann^{*1}

¹Department of Nuclear Medicine and Clinical Molecular Imaging, University Hospital Tuebingen, Tuebingen, Germany; ²Department of Women's Health, University Hospital Zurich, Zurich, Switzerland; ³Department of Diagnostic and Interventional Radiology, University Hospital Tuebingen, Tuebingen, Germany; ⁴Department of Women's Health, University Hospital Tuebingen, Tuebingen, Germany; ⁵iFIT Cluster of Excellence, Eberhard Karls University Tuebingen, Tuebingen, Germany; and ⁶German Cancer Consortium, Partner Site Tuebingen, Germany

Lymph node metastasis (LNM) is present in a minority of patients with early stages of cervical carcinomas. As conventional imaging including PET/CT has shown limited sensitivity, systematic lymphadenectomies are often conducted for staging purposes. Therefore, the aim of this prospective study was to analyze the impact of ¹⁸F-FDG PET/MRI in addition to sentinel lymph node (SLN) biopsy on lymph node (LN) status. **Methods:** Forty-two women with an initial diagnosis of Fédération Internationale de Gynécologie et d'Obstétrique (FIGO) IA–IIB cervical carcinoma were included between March 2016 and April 2019. Each patient underwent preoperative whole-body ¹⁸F-FDG PET/MRI and SLN imaging with SPECT/CT after intracervical injection of ^{99m}Tc-labeled nanocolloid. Systematic lymphadenectomy and SLN biopsy served as the reference standard. Staging using PET/MRI was performed by nuclear medicine and radiology experts working in consensus. **Results:** One patient was excluded from surgical staging because of liver metastases newly diagnosed on PET/MRI. The overall prevalence of LNM in the remaining 41 patients was 29.3% (12/41). Five of 12 patients with LNM had solely small metastases with a maximum diameter of 5 mm. The consensus interpretation showed PET/MRI to have a specificity of 100% (29/29; 95% CI, 88.3%–100%) for LNM staging but a low sensitivity, 33.3% (4/12; 95% CI, 12.8%–60.9%). LN size was the most important factor for the detectability of metastases, since only LNMs larger than 5 mm could be identified by PET/MRI (sensitivity, 57.1% for >5 mm and 0% for ≤5 mm). Paraaortic LNM was evaluated accurately in 3 of the 4 patients with paraaortic LN metastasis. SLNs were detectable by SPECT/CT in 82.9% of the patients or 69.0% of the hemipelvises. In cases with an undetectable SLN on SPECT/CT, the malignancy rate was considerably higher (31.2% vs. 19.3%). The combination of PET/MRI and SLN SPECT/CT improved the detection of pelvic LNM from 33.3% to 75%. **Conclusion:** ¹⁸F-FDG PET/MRI is a highly specific N-staging method and improves LNM detection. Because of the limited sensitivity in frequently occurring small LNMs, PET/MRI should be combined with SLN mapping. The proposed combined protocol helps to decide whether extensive surgical staging is necessary in patients with FIGO I/II cervical cancer.

Key Words: ¹⁸F-FDG PET/MRI; ^{99m}Tc-nanocolloid SPECT/CT; sentinel node; cervical carcinoma; combined protocol

Received Sep. 11, 2020; revision accepted Dec. 4, 2020.

For correspondence or reprints, contact Christian la Fougère (christian.lafougere@med.uni-tuebingen.de).

*Contributed equally to this work.

Published online January 28, 2021.

COPYRIGHT © 2021 by the Society of Nuclear Medicine and Molecular Imaging.

J Nucl Med 2021; 62:1062–1067

DOI: 10.2967/jnumed.120.255919

Staging of cervical carcinoma is still based on clinical criteria and surgical specimens according to the Fédération Internationale de Gynécologie et d'Obstétrique (FIGO) classification (1). However clinical staging becomes less accurate with increasing tumor stage, with a reported under- or overstaging in up to 65% of patients (2–5).

As the presence of lymph node metastasis (LNM) is the most important prognostic factor in early stages (4,6–11), accurate staging is essential. Therefore, imaging methods are increasingly used in addition to clinical staging and are gradually being mentioned in current guidelines (1,4,6,10).

Unfortunately, LNM can occur in any stage of cervical carcinoma, with an increasing prevalence from 15% in early-stage tumors to about 35% in carcinomas larger than 4 cm (10,12,13). Therefore, pelvic systematic lymphadenectomy—sometimes extended to para-aortic lymph nodes (LNs)—remains the gold standard for N-staging (1,4,6,10). Regrettably, this procedure is often associated with high morbidity and seems to be very invasive for the low prevalence of LNM in early tumor stages (1,4,6,10,14).

To minimize overtreatment, sentinel LN (SLN) biopsy is increasingly performed in several centers and has been established by guidelines for cervical cancer staging (4,6). The minimally invasive SLN biopsy is usually performed after an intracervical injection of fluorescent dye or ^{99m}Tc labeled nanocolloid, whereby the combination of both is superior (10,15).

Furthermore, a targeted removal of only a few LNs enables a more intensive histopathologic processing, by ultrastaging protocol. By means of ultrastaging, the LN is lamellated more finely and, if necessary, processed immunohistochemically so that even single tumor cells can be detected (16). This procedure results in a higher detection rate (upstaging in 5%–15% of patients) of micrometastases (16), which were shown to have an impact on recurrence probability and overall survival (17).

As a noninvasive imaging method that was first introduced for local tumor staging (5), MRI revealed its advantages quickly for pelvic LNs, with a high pooled specificity of about 95% but low sensitivity of about 55% (3,6,10,18).

Moreover, ¹⁸F-FDG PET enables whole-body staging, with excellent results in local tumor staging and in the detection of metastases (19–21). However, the use of PET/CT is still controversial (4,10,18).

According to the National Comprehensive Cancer Network guidelines, PET/CT can be considered for primary staging starting from FIGO IB (4), whereas the European Society of Medical Oncologists guidelines recommend PET/CT in locally advanced disease (10).

On the basis of the current data, whole-body ¹⁸F-FDG PET/MRI has the potential to combine the strength of MRI for locoregional tumors and LN staging with the capability of whole-body PET to exclude distant metastases, including lung metastases, in a 1-stop shop (19).

We hypothesize that a combined protocol of ¹⁸F-FDG PET/MRI and SPECT/CT for SLN detection could be an accurate, minimally invasive whole-body staging procedure. In particular, ultrastaging in the SLN enables the detection of micrometastases and isolated tumor cells that can hardly be visualized by any imaging method (16). A more precise preoperative staging could save patients with nonresectable N- or M-stage from a possibly unnecessary surgery.

MATERIALS AND METHODS

Forty-two patients with histopathologically confirmed cervical carcinoma and clinically determined stage FIGO IA to IIB were consecutively enrolled into this prospective study. The study was approved by the institutional review board (registry no. 173/2015BO01) and is listed in the German Clinical Trial Register (DRKS identifier DRKS00014346) (22). All patients gave written informed consent.

Each patient underwent whole-body ¹⁸F-FDG PET/MRI, preoperative SLN mapping with SPECT/CT, intraoperative SLN detection with a γ -probe, and surgical staging between March 2016 and April 2019.

There was 1 dropout due to newly diagnosed liver metastases on PET/MRI (clinical stage: pT1b1,L1,V0,R1,G1; final stage after PET/MRI: T2b,N1,M1). Two patients (3 hemipelvs) were excluded from the evaluations with histologic correlation (1 patient without pelvic LN extraction, 1 hemipelvis due to unclear anatomic allocation). Detailed patient characteristics are presented in Table 1.

PET/MRI Protocol

A Biograph mMR (Siemens Healthineers) was used for the PET/MRI acquisition, which started 65.3 ± 13.9 min after injection of 238.3 ± 14.8 MBq of ¹⁸F-FDG. To minimize intestinal movement, 20 mg of intravenous butylscopolamine bromide were administered concomitantly with the radiotracer injection unless contraindicated. All patients fasted for at least 8 h, and the blood sugar level at injection was below 140 mg/dL. The minimum acquisition time per bed position was 4 min. Detailed MRI parameters are listed in detail in Supplemental Table 1 (supplemental materials are available at <http://jnm.snmjournals.org>). PET/MR images were evaluated in consensus by board-certified radiology and nuclear medicine specialists with at least 8 y of experience in PET and MRI.

TABLE 1
Patient Characteristics (n = 41)

| Characteristic | Average \pm SD | Range |
|---|------------------|------------|
| Age at PET/MRI (y) | 48.1 \pm 12.2 | 28.1–80.9 |
| Patient size (cm) | 166 \pm 6.7 | 152–187 |
| Patient weight (kg) | 70.8 \pm 17.0 | 44.0–117.0 |
| Body mass index (kg/m ²) | 25.8 \pm 6.0 | 15.2–40.0 |
| Time between PET/MRI and LN histology (d) | 22.4 \pm 15.7 | 1–71 |

SLN Injection Technique

Approximately 200 MBq of ^{99m}Tc-nanocolloid (Nanocoll; GE Healthcare) diluted with 0.9% NaCl to a volume of 0.8 mL were injected intracervically, evenly distributed at the 3-, 6-, 9-, and 12-o'clock positions.

SLN SPECT/CT

LN mapping was performed 3–5 h after ^{99m}Tc-nanocolloid injection. All patients were scanned on a hybrid SPECT/CT device (Discovery 670 Pro; GE Healthcare) including an area from pelvis to caudal liver with the 2 camera heads in H-Mode. The SPECT acquisition parameters were an energy window of $140.5 \text{ keV} \pm 10\%$, a 128×128 matrix, 30 angular steps with a 6° interval, an acquisition time of 15 min/step, and a pixel size of 4.42×4.42 mm. SPECT data were reconstructed using an ordered-subsets expectation maximization iterative protocol (2 iterations, 10 subsets).

The technical parameters of the 16-slice CT scanner were a gantry rotation speed of 0.8 s and a table feed of 20 mm/gantry rotation. CT scans were obtained with a dose modulation system (120 kV, 10–80 mAs [OptiDose; GE Healthcare]). A contrast agent (90 mL of Ultravist 370; Bayer Vital GmbH) was injected unless contraindicated.

The SLN SPECT/CT was analyzed by 2 nuclear medicine physicians with more than 10 y of experience in pelvic SLN imaging. An SLN was defined as focal activity enrichment on SPECT in a plausible anatomic region. SLN mapping was defined as successful if at least 1 SLN per hemipelvis was clearly detectable.

SLN Biopsy

Surgical staging was performed laparoscopically the day after ^{99m}Tc-nanocolloid injection. Blue dye or indocyanine green was injected intracervically at the 3- and 9-o'clock positions (0.2 mL per injection) before surgery.

SLNs were localized and identified intraoperatively either by direct visualization or using a laparoscopic γ -probe (Neoprobe, models 1017 and 1100; Devicor Medical Products, Inc.), resected separately, assigned meticulously, and sent for rapid tissue sectioning.

All patients underwent bilateral systematic lymphadenectomy with resection of SLNs and of macroscopically suggestive LNs. Additional paraaortic LNs were removed in cases of higher tumor stages or after histopathologic proof of LNM by frozen sectioning. Ultrastaging was performed for the SLN, with complete preparation of the entire LN with 200- μ m slices.

Statistical Analysis

Statistical analysis was performed with SPSS Statistics software, version 25.0 (IBM Inc.), and MedCalc software, version 19.3. Test performance was calculated with 4-fold tables. The Fisher exact test (2-tailed) was used to verify significant differences in the prevalence of LNM. A *P* value of less than 0.05 was considered statistically significant.

RESULTS

Tumor Histology and Prevalence of LNM

Almost every tumor stage from pT1a to pT2b was represented in this cohort (Table 2). Tumor grade was balanced between G1/G2 and G3 (G1: *n* = 4, G2: *n* = 17, G3: *n* = 20). In 1 case, because a peritoneal involvement could not be ruled out histologically (pTx), the clinical assessment of the tumor border (cT2b, M1 [peritoneum]) was applied. The prevalence of LNM was 29.3% per patient (12/41) and 22.8% per hemipelvis (18/79). Five of 12 patients presented with solely small LNMs at a maximum diameter of 5 mm.

The presence of LNM was significantly higher in pT2 (63.6%) than pT1 stages (13.8%, *P* < 0.05). No LNM was found with G1 tumors or T1a tumor stages.

TABLE 2
Distribution of Patients by Tumor Stage

| Tumor stage | | Number of patients | | |
|-------------|------|--------------------|-------|--------|
| | | G1 | G2 | G3 |
| pT1 | pT1a | 1 (0) | 3 (0) | 1 (0) |
| | pT1b | 2 (0) | 8 (2) | 14 (2) |
| | pT1c | — | — | — |
| pT2 | pT2a | — | 1 (0) | — |
| | pT2b | 1 (0) | 3 (3) | 6 (4) |
| pTx (cT2b) | | — | — | 1 (1) |

Data in parentheses are patients with pelvic LNM. Subgroups of tumor stages are summarized.

Paraortic LNM was strictly associated with higher tumor stage and grade (3/4 pT2b [1xG1, 2xG2], 1/4 pTx [G3]). All patients with paraortic LNM presented with LNM in both hemipelvises.

¹⁸F-FDG PET/MRI

The prospective reading of PET/MRI as an expert consensus demonstrated a very high specificity for pelvic LN staging in both patient-based (29/29 [100%]; 95% CI, 88.1%–100%) and hemipelvis-based (61/61 [100%]; 95% CI, 94.1%–100%) analyses.

However, sensitivity for pelvic LNM detection was considerably limited (patient-based analysis: 4/12 [33.3%]; 95% CI, 9.9%–65.1%; hemipelvis-based analysis: 5/18 [27.8%]; 95% CI, 9.7%–53.5%). Here, the size of the LN played a decisive role for LNM detection by PET/MRI, as it enabled detection of only those LNMs larger than 5 mm (4/7; 57%); no LNMs 5 mm or smaller (0/5) were found.

Thus, the accuracy, PPV, and NPV of PET/MRI for LNM detection were 80.5% (33/41; 95% CI, 65.1%–91.2%), 100% (4/4), and 78.4% (29/37), respectively, on a patient level and 83.5% (66/79; 95% CI, 73.5–90.9), 100% (5/5), and 82% (61/74), respectively, on a hemipelvis level.

Tumor grade had no significant impact on detectability on PET/MRI, as the distribution of G3 and G2 status was comparable in detectable LNMs (G3: *n* = 2, G2: *n* = 2) and nondetectable LNMs (G3: *n* = 4, G2: *n* = 4).

Pelvic lymphadenectomy was extended to a paraortic LN sampling in 16 of 41 patients. Four of these 16 presented with paraortic LNMs at histology. These paraortic LNMs were rated correctly by PET/MRI in 3 of 4 patients, resulting in a sensitivity of 75% (95% CI, 19.4%–99.4%), a specificity of 100% (12/12; 95% CI, 73.5%–100%), and an accuracy of 94% (15/16; 95% CI, 66.8%–99.8%). All detected paraortic LNMs had diameters between 8 and 45 mm and were related to pT2b, G3 tumors. The single missed LNM was from a G2 tumor and had a maximal diameter of 7 mm.

SLN Detection

SPECT/CT detected at least 1 SLN in 82.9% of all patients (34/41) and in 70.7% of hemipelvises (58/82). SLNs in both hemipelvises were detectable in 61.0% of patients (25/41). The rate of detecting paraortic SLNs was substantially lower (31.7%, 13/41). In 1 patient, SLNs were visualized solely by dye, increasing the overall detection rate to 85.4% (35/41) on a patient-based level.

The presence of LNM was higher in patients or hemipelvises without a detectable SLN on SPECT/CT (50% [3/6] or 31.2% [7/22],

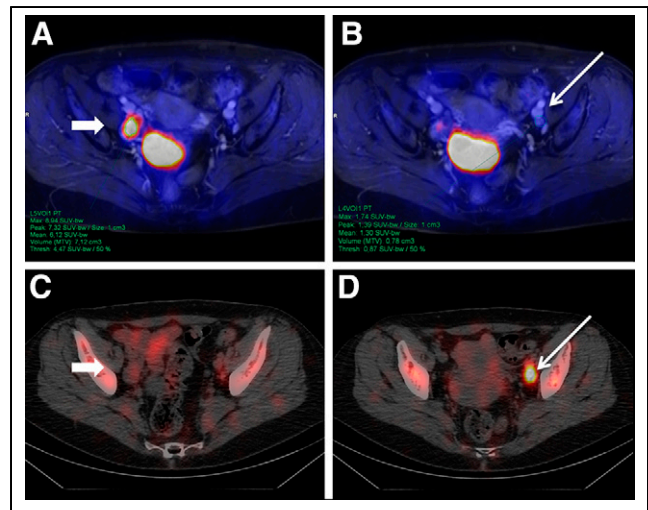


FIGURE 1. A 58-year-old woman with newly diagnosed T2b G3 cervical carcinoma. PET/MRI (top row) detected enlarged LN in right hemipelvis (A, arrow) with intense ¹⁸F-FDG uptake. In contrast, ^{99m}Tc-nanocolloid SPECT/CT showed clearly definable SLN in left hemipelvis (D, arrow) with benign characteristics on PET/MRI (B). After surgery, 1 LN in right hemipelvis (A and C) was confirmed as LNM. SLN on left (B and D) had benign histology.

respectively) than when an SLN was detectable (23.5% [8/34] or 19.3% [11/57], respectively). A representative case is shown in Figure 1. However, the difference was not significant on a patient or hemipelvis level (*P* = 0.32 and 0.25, respectively). Only 1 of 4 patients with paraortic LNM showed corresponding SLNs on SPECT/CT.

To analyze the representativeness of SLN biopsy for assessment of N-status on a hemipelvis level, we performed an additional sub-analysis on SLNs that were clearly assignable on SPECT/CT and on γ -probe visualization (44 SLNs assignable in 35 hemipelvises of 24 patients). The prevalence of malignancy was 22.9% (8/35), and sensitivity was 87.5% (7/8; 95% CI, 47.4%–99.7%); specificity, 100% (27/27; 95% CI, 87.2%–100%); accuracy, 97% (34/35; 95% CI, 85.1–99.9); PPV, 100% (7/7); and NPV, 96.4% (27/28).

Combined PET/MRI and SLN Protocol

Combining ¹⁸F-FDG PET/MRI and SLN imaging improved the detection rate of LNM substantially from 33.3% to 75.0% on a patient-based level and from 27.8% to 66.7% on a hemipelvis level. In return, PET/MRI was superior to SLN imaging for the detection of paraortic LNM. Further details are shown in Table 3.

In a subanalysis of 28 patients with tumors 4 cm or smaller, no parametrial invasion, and no enlarged LNMs, SLN imaging detected LNM in 3 of 3 patients or 3 of 4 hemipelvises. Implementing additional PET data could not improve LNM detection (0/3) in this small subgroup with metastases of 0.5–4 mm.

A representative example of the synergies between the 2 modalities is presented in Figure 2. However, our data imply that PET/MRI cannot predict LN status precisely in cases of failed SLN detection (Fig. 3).

DISCUSSION

To our knowledge, this was the first prospective study on a combined protocol of ¹⁸F-FDG PET/MRI and SLN SPECT/CT for the purpose of LN staging in patients with cervical carcinoma. The data suggest that PET/MRI has a high specificity in LN

TABLE 3
 Detection Rate of LNM in ¹⁸F-FDG PET/MRI, SLN SPECT/CT, and Combined Protocol

| Parameter | PET/MRI | SLN | PET/MRI + SLN |
|----------------------|--------------|---------------|---------------|
| Per patient | 33.3% (4/12) | 66.7% (8/12) | 75.0% (9/12) |
| ≤pT2a1 and N0 in MRI | 0% (0/3) | 100% (3/3) | 100% (3/3) |
| ≥pT2a2 | 14.3% (1/7) | 42.9% (3/7) | 42.9% (3/7) |
| Hemipelvis | 27.8% (5/18) | 61.1% (11/18) | 66.7% (12/18) |
| ≤pT2a1 and N0 in MRI | 0% (0/4) | 75.0% (3/4) | 75.0% (3/4) |
| ≥pT2a2 | 18.2% (2/11) | 45.5% (5/11) | 54.5% (6/11) |
| Paraortic LNM | 75% (3/4) | 25% (1/4) | 75% (3/4) |

staging but only a limited sensitivity because of the presence of LNMs smaller than 5 mm, which seem to occur frequently in early-stage tumors.

In contrast to intravenously injected tracers and contrast media, the SLN technique provides decisive information about lymphatic drainage of the tumor and identifies the LN with the highest risk for metastasis independent of its size. Thus, the combination of metabolic and morphologic information from PET/MRI with functional information from lymph drainage resulted in a significant improvement in sensitivity and detection rate.

Diagnostic Power of PET/MRI

Detection of small metastases is known to be a major challenge for PET. However, the sensitivity in our study was lower than in earlier PET/CT (44%) and PET/MRI studies (33% vs. 44%–88%) (20,21,23,24). This discrepancy might be explained by the high rate of small LNMs compared with previous studies (20,21,23,24),

which might be due to the defined cohort of solely FIGO I–II stage, exhibiting a reported prevalence of micrometastases of more than 40% (25,26).

In addition, this was the first PET study on this topic implementing ultrastaging as gold standard, which increases the detection of micrometastases by up to 28% (16). In our study, the implementation of ultrastaging enabled the detection of micrometastases down to 0.5 mm. As the partial-volume effect increases with decreasing lesion size, PET has a poor sensitivity in the lower millimeter range, thus missing smaller metastases (27,28). Consequently, it can be hypothesized that studies without ultrastaging as the gold standard might overrate the sensitivity of PET.

Unfortunately, MRI was only able to compensate for the difficulties of PET to a limited extent, especially in small metastases. Because of the limited spatial resolution of diffusion-weighted images, only LN larger than 5 mm were evaluated sufficiently on apparent-diffusion-coefficient images (29,30). The described improvement in LNM detection by calculating the ratio of apparent-diffusion-coefficient LN to primary tumor (29) was not applicable to our cohort, as most of the patients underwent diagnostic conization before PET/MRI.

Contrary to the limited sensitivity, the specificity of PET/MRI was very high in the assessment of LNM. This high specificity refers not only to pelvic LNM but also to paraortic LNM and is

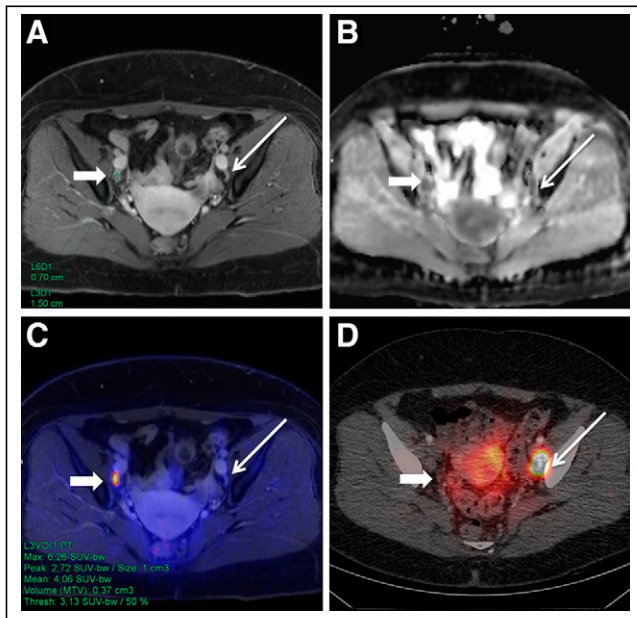


FIGURE 2. A 55-year-old woman with initial diagnosis of T1b G2 cervical carcinoma. PET/MRI showed slightly enlarged contrast-enhanced LN in right hemipelvis (A, thick arrow) with diffusion restriction in apparent-diffusion-coefficient map (B) and focal ¹⁸F-FDG uptake in PET-fused image (C) but no ^{99m}Tc-nanocolloid uptake on SPECT/CT (D). In contrast, SLN in left hemipelvis (C, thin arrow) was not suggestive on PET/MR images (A–C). Both LNMs were removed and histologically confirmed as LNMs.

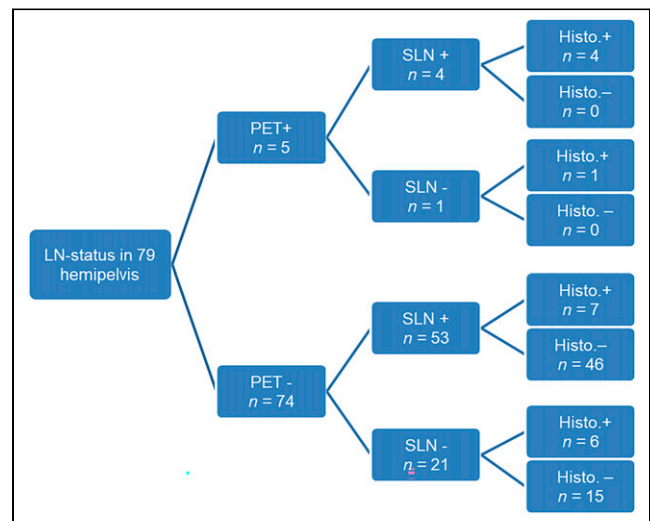


FIGURE 3. Overview of distribution of LNM depending on PET/MRI findings and detectability of SLNs.

comparable to previous PET/CT and PET/MRI studies with reported specificities of 84%–94% (20,21,23,24).

As the presence of pelvic or paraaortic LNM results in an upstaging to FIGO IIIB or FIGO IVB, PET/MRI can have a major impact on clinical management. For example, the histologic confirmation of a PET-positive paraaortic LNM via minimally invasive LN biopsy could shift the patient's treatment from an unnecessary and stressful hysterectomy to radiochemotherapy.

Furthermore, MRI has the potential to detect infiltration of the pelvic wall, which is important for the differentiation between T3a and T3b or FIGO IIIA and FIGO IIIB stage and has accuracy equal to or better than that of clinical staging (5,24,31).

SLN Detection Rate

Our study confirms previous work that stated that the removal of single SLNs is representative of pelvic LN status (15,32). The presence of pelvic LNM was correctly demonstrated by SLN removal in all our patients with successful SPECT/CT-confirmed radioactive SLN labeling.

Our SLN detection rate on SPECT/CT was slightly lower than described in the current literature (33,34). As higher tumor stages and LNM prevalence are associated with a significantly lower SLN detection rate (33), the composition of this cohort—with higher tumor stages than in other SLN studies—might be a potential explanation. Current data indicate an up to 50% higher risk for LNM in cases of failed SLN detection on SPECT/CT (33,34). Although the significance level was not reached because of the limited number of LNs, it might be hypothesized that missed SLN detection on imaging is not necessarily indicative of an insufficient injection. Rather, metastatic tissue might inhibit lymph drainage or disrupt the filtering function of involved LNs.

Combination of PET/MRI and SLN SPECT/CT

The combination of PET/MRI and SLN SPECT/CT resulted in the highest detection rate for LNM, and the additional value of PET/MRI increases with advanced tumor stage and parametrial invasion. However, PET/MRI could not improve N-staging in cases of small tumors restricted to the cervix; in such cases, the false-negative rate has been described as being below 0.1% if there is successful SLN mapping and no suggestive LNs on MRI (32). Thus PET/MRI seems to contribute little to this specific patient group. In clinical practice, however, successful SLN marking and the final tumor stage often become apparent only during surgery. If whole-body imaging is omitted when there is a clinically assumed low T-stage, paraaortic LNM or distant metastases may be missed, as demonstrated here by a patient with pT1 tumor but liver metastases.

The fact that ¹⁸F-FDG PET/MRI contributes to the detection of LNMs might be explained by loss of colloid avidity. In addition, the SLN technique is independent of LN size and thus enables the biopsy-based detection of small LNMs beyond the resolution limit of PET and MRI, improving sensitivity considerably.

The detection rate of paraaortic LNs using SPECT/CT was higher in the current study than in previous studies (35,36) but was not sufficient as a stand-alone method for reliable assessment of the paraaortic status.

Our results demonstrate that PET/MRI has the potential to identify paraaortic LNMs; however, the statistical power is still limited (23,24). As imaging with ¹⁸F-FDG allows assessment of all organ systems, a full-body PET/MRI staging can be performed in 30–40 min.

Limitations

The limitation of this study is that the data represent an interim evaluation of an ongoing prospective study. Although the study covers the largest collective to date, the available data tend to indicate trends in some issues. For confirmation of these trends, more data are needed.

So far, the evaluation has been conducted at only a patient level and a hemipelvis level. However, because of the limited sensitivity of PET/MRI, further evaluation of the multiparametric data at an LN level is necessary. Thus, a larger study including a higher number of LNMs is desirable to further evaluate PET/MRI in this entity.

CONCLUSION

¹⁸F-FDG PET/MRI is a highly specific method in LN staging that improves LNM detection. Because of the limited sensitivity in frequently occurring small LNMs, PET/MRI should be combined with SLN SPECT/CT. The combined protocol helps to decide whether extensive surgical staging is needed in patients with FIGO I/II cervical cancer.

DISCLOSURE

This work was funded by the Deutsche Forschungsgemeinschaft (DFG, German Research Foundation) under Germany's Excellence Strategy (EXC 2180-390900677). No other potential conflict of interest relevant to this article was reported.

KEY POINTS

QUESTION: Does the combination of ¹⁸F-FDG PET/MRT and SLN SPECT/CT improve LN staging in FIGO I/II cervical carcinoma?

PERTINENT FINDINGS: In this prospective study, PET/MRI exhibited a specificity of 100% but limited sensitivity of 33%. The combination of PET/MRI and SPECT/CT-guided SLN biopsy increased the detection rate of LNM to 75%.

IMPLICATIONS FOR PATIENT CARE: ¹⁸F-FDG PET/MRI can save metastasized patients from unnecessary surgery but should be combined with SLN biopsy because of its limited sensitivity in frequently occurring small metastases.

REFERENCES

1. Bhatla N, Berek JS, Cuello Fredes M, et al. Revised FIGO staging for carcinoma of the cervix uteri. *Int J Gynaecol Obstet.* 2019;145:129–135.
2. Lagasse LD, Creasman WT, Shingleton HM, Ford JH, Blessing JA. Results and complications of operative staging in cervical cancer: experience of the Gynecologic Oncology Group. *Gynecol Oncol.* 1980;9:90–98.
3. Selman TJ, Mann C, Zamora J, Appleyard TL, Khan K. Diagnostic accuracy of tests for lymph node status in primary cervical cancer: a systematic review and meta-analysis. *CMAJ.* 2008;178:855–862.
4. Koh WJ, Abu-Rustum NR, Bean S, et al. Cervical cancer, version 3.2019, NCCN clinical practice guidelines in oncology. *J Natl Compr Canc Netw.* 2019;17:64–84.
5. Thomeer MG, Gerestein C, Spronk S, van Doom HC, van der Ham E, Hunink MG. Clinical examination versus magnetic resonance imaging in the pretreatment staging of cervical carcinoma: systematic review and meta-analysis. *Eur Radiol.* 2013;23:2005–2018.
6. *S3 Guideline for Diagnostics, Therapy and Aftercare of Patients with Cervical Cancer: Long Version, 1.0—AWMF Registration Number 032/033OL* [in German]. AWMF Online; 2014. https://www.leitlinienprogramm-onkologie.de/fileadmin/user_upload/Downloads/Leitlinien/Zervixkarzinom/LL_Zervixkarzinom_Langversion_1.0.pdf. Accessed May 27, 2021.
7. Tanaka Y, Sawada S, Murata T. Relationship between lymph node metastases and prognosis in patients irradiated postoperatively for carcinoma of the uterine cervix. *Acta Radiol Oncol.* 1984;23:455–459.

8. Fuller AF Jr, Elliott N, Kosloff C, Hoskins WJ, Lewis JL Jr. Determinants of increased risk for recurrence in patients undergoing radical hysterectomy for stage IB and IIA carcinoma of the cervix. *Gynecol Oncol*. 1989;33:34–39.
9. Kim SM, Choi HS, Byun JS. Overall 5-year survival rate and prognostic factors in patients with stage IB and IIA cervical cancer treated by radical hysterectomy and pelvic lymph node dissection. *Int J Gynecol Cancer*. 2000;10:305–312.
10. Marth C, Landoni F, Mahner S, et al.; ESMO Guidelines Committee. Cervical cancer: ESMO clinical practice guidelines for diagnosis, treatment and follow-up. *Ann Oncol*. 2017;28(suppl 4):iv72–iv83.
11. Pieterse QD, Kenter GG, Gaarenstroom KN, et al. The number of pelvic lymph nodes in the quality control and prognosis of radical hysterectomy for the treatment of cervical cancer. *Eur J Surg Oncol*. 2007;33:216–221.
12. Kadkhodayan S, Hasanzadeh M, Treglia G, et al. Sentinel node biopsy for lymph nodal staging of uterine cervix cancer: a systematic review and meta-analysis of the pertinent literature. *Eur J Surg Oncol*. 2015;41:1–20.
13. SiSaia P, Creasman W, Mannel R, Scott D. *Clinical Gynecologic Oncology*. Vol 9: Elsevier; 2017:38–101.
14. Holman LL, Levenback CF, Frumovitz M. Sentinel lymph node evaluation in women with cervical cancer. *J Minim Invasive Gynecol*. 2014;21:540–545.
15. van de Lande J, Torrenza B, Raijmakers PG, et al. Sentinel lymph node detection in early stage uterine cervix carcinoma: a systematic review. *Gynecol Oncol*. 2007;106:604–613.
16. Bats AS, Mathevet P, Buenerd A, et al. The sentinel node technique detects unexpected drainage pathways and allows nodal ultrastaging in early cervical cancer: insights from the multicenter prospective SENTICOL study. *Ann Surg Oncol*. 2013;20:413–422.
17. Marchiolé P, Buenerd A, Benchaib M, Nezhat K, Dargent D, Mathevet P. Clinical significance of lympho vascular space involvement and lymph node micrometastases in early-stage cervical cancer: a retrospective case-control surgico-pathological study. *Gynecol Oncol*. 2005;97:727–732.
18. Choi HJ, Ju W, Myung SK, Kim Y. Diagnostic performance of computer tomography, magnetic resonance imaging, and positron emission tomography or positron emission tomography/computer tomography for detection of metastatic lymph nodes in patients with cervical cancer: meta-analysis. *Cancer Sci*. 2010;101:1471–1479.
19. Li K, Sun H, Guo Q. Combinative evaluation of primary tumor and lymph nodes in predicting pelvic lymphatic metastasis in early-stage cervical cancer: a multi-parametric PET-CT study. *Eur J Radiol*. 2019;113:153–157.
20. Stecco A, Buemi F, Cassara A, et al. Comparison of retrospective PET and MRI-DWI (PET/MRI-DWI) image fusion with PET/CT and MRI-DWI in detection of cervical and endometrial cancer lymph node metastases. *Radiol Med (Torino)*. 2016;121:537–545.
21. Kim SK, Choi HJ, Park SY, et al. Additional value of MR/PET fusion compared with PET/CT in the detection of lymph node metastases in cervical cancer patients. *Eur J Cancer*. 2009;45:2103–2109.
22. DRKS-ID: DRKS00014346. German Clinical Trials Register website. https://www.drks.de/drks_web/navigate.do?navigationId=trial.HTML&TRIAL_ID=DRKS00014346. Accessed April 7, 2021.
23. Sarabhai T, Schaarschmidt BM, Wetter A, et al. Comparison of ¹⁸F-FDG PET/MRI and MRI for pre-therapeutic tumor staging of patients with primary cancer of the uterine cervix. *Eur J Nucl Med Mol Imaging*. 2018;45:67–76.
24. Grueneisen J, Schaarschmidt BM, Heubner M, et al. Integrated PET/MRI for whole-body staging of patients with primary cervical cancer: preliminary results. *Eur J Nucl Med Mol Imaging*. 2015;42:1814–1824.
25. Lentz SE, Munderspach LI, Felix JC, Ye W, Groshen S, Amezcuca CA. Identification of micrometastases in histologically negative lymph nodes of early-stage cervical cancer patients. *Obstet Gynecol*. 2004;103:1204–1210.
26. Juretzka MM, Jensen KC, Longacre TA, Teng NN, Husain A. Detection of pelvic lymph node micrometastasis in stage IA2-IB2 cervical cancer by immunohistochemical analysis. *Gynecol Oncol*. 2004;93:107–111.
27. Bellevue D, Blanc Fournier C, Switers O, et al. Staging the axilla in breast cancer patients with ¹⁸F-FDG PET: how small are the metastases that we can detect with new generation clinical PET systems? *Eur J Nucl Med Mol Imaging*. 2014;41:1103–1112.
28. Cysouw MCF, Kramer GM, Hoekstra OS, et al. Accuracy and precision of partial-volume correction in oncological PET/CT studies. *J Nucl Med*. 2016;57:1642–1649.
29. Lin G, Ho KC, Wang JJ, et al. Detection of lymph node metastasis in cervical and uterine cancers by diffusion-weighted magnetic resonance imaging at 3T. *J Magn Reson Imaging*. 2008;28:128–135.
30. Roy C, Bierry G, Matau A, Bazille G, Pasquali R. Value of diffusion-weighted imaging to detect small malignant pelvic lymph nodes at 3 T. *Eur Radiol*. 2010;20:1803–1811.
31. Ozsarlak O, Tjalma W, Schepens E, et al. The correlation of preoperative CT, MR imaging, and clinical staging (FIGO) with histopathology findings in primary cervical carcinoma. *Eur Radiol*. 2003;13:2338–2345.
32. Tax C, Rovers MM, de Graaf C, Zusterzeel PL, Bekkers RL. The sentinel node procedure in early stage cervical cancer, taking the next step; a diagnostic review. *Gynecol Oncol*. 2015;139:559–567.
33. Balaya V, Bresset A, Guani B, et al. Risk factors for failure of bilateral sentinel lymph node mapping in early-stage cervical cancer. *Gynecol Oncol*. 2020;156:93–99.
34. Cibula D, Kuzel D, Slama J, et al. Sentinel node (SLN) biopsy in the management of locally advanced cervical cancer. *Gynecol Oncol*. 2009;115:46–50.
35. Diaz-Feijoo B, Perez-Benavente MA, Cabrera-Diaz S, et al. Change in clinical management of sentinel lymph node location in early stage cervical cancer: the role of SPECT/CT. *Gynecol Oncol*. 2011;120:353–357.
36. Ogawa S, Kobayashi H, Amada S, et al. Sentinel node detection with ^{99m}Tc phytate alone is satisfactory for cervical cancer patients undergoing radical hysterectomy and pelvic lymphadenectomy. *Int J Clin Oncol*. 2010;15:52–58.